

Article

Investigation of the Historical Trends and Variability of Rainfall Patterns during the March–May Season in Rwanda

Constance Uwizewe ^{1,2,3,4,5} , Li Jianping ^{1,2,3,4,6,*}, Théogène Habumugisha ^{7,8}  and Ahmad Abdullahi Bello ^{1,2,3,4}

¹ Frontiers Science Center for Deep Ocean Multispheres and Earth System, Ocean University of China, Qingdao 266100, China

² Key Laboratory of Physical Oceanography, Ministry of Education, Ocean University of China, Qingdao 266100, China

³ College of Oceanography and Atmospheric Sciences, Ocean University of China, Qingdao 266100, China

⁴ Academy of the Future Ocean, Ocean University of China, Qingdao 266100, China

⁵ Rwanda Meteorology Agency, Kigali P.O. Box 898, Rwanda

⁶ Laboratory for Ocean Dynamics and Climate, Pilot National Laboratory for Marine Science and Technology, Qingdao 266237, China

⁷ Key Laboratory of Urban Environment and Health, Institute of Urban Environment, Chinese Academy of Sciences, Xiamen 361021, China

⁸ University of Chinese Academy of Sciences, Beijing 10049, China

* Correspondence: ljp@ouc.edu.cn

Abstract: This study explores the spatiotemporal variability and determinants of rainfall patterns during the March to May (MAM) season in Rwanda, incorporating an analysis of teleconnections with oceanic–atmospheric indices over the period 1983–2021. Utilizing the Climate Hazards Group Infrared Precipitation with Stations (CHIRPS) dataset, the study employs a set of statistical tools including standardized anomalies, empirical orthogonal functions (EOF), Pearson correlation, the Mann–Kendall (MK) trend test, and Sen’s slope estimator to dissect the intricacies of rainfall variability, trends, and their association with large-scale climatic drivers. The findings reveal a distinct southwest to northwest rainfall gradient across Rwanda, with the MK test signaling a decline in annual precipitation, particularly in the southwest. The analysis for the MAM season reveals a general downtrend in rainfall, attributed in part to teleconnections with the Indian Ocean Sea surface temperatures (SSTs). Notably, the leading EOF mode for MAM rainfall demonstrates a unimodal pattern, explaining a significant 51.19% of total variance, and underscoring the pivotal role of atmospheric dynamics and moisture conveyance in shaping seasonal rainfall. The spatial correlation analysis suggests a modest linkage between MAM rainfall and the Indian Ocean Dipole, indicating that negative (positive) phases are likely to result in anomalously wet (dry) conditions in Rwanda. This comprehensive assessment highlights the intricate interplay between local rainfall patterns and global climatic phenomena, offering valuable insights into the meteorological underpinnings of rainfall variability during Rwanda’s critical MAM season.

Keywords: Rwanda; rainfall; CHIRPS; teleconnections; variability; trends; dipole; atmosphere



Citation: Uwizewe, C.; Jianping, L.; Habumugisha, T.; Bello, A.A. Investigation of the Historical Trends and Variability of Rainfall Patterns during the March–May Season in Rwanda. *Atmosphere* **2024**, *15*, 609. <https://doi.org/10.3390/atmos15050609>

Academic Editor: Mario Marcello Miglietta

Received: 20 March 2024

Revised: 9 May 2024

Accepted: 15 May 2024

Published: 17 May 2024



Copyright: © 2024 by the authors. Licensee MDPI, Basel, Switzerland. This article is an open access article distributed under the terms and conditions of the Creative Commons Attribution (CC BY) license (<https://creativecommons.org/licenses/by/4.0/>).

1. Introduction

Rainfall stands as a pivotal climatic variable, significantly influencing the ramifications of climate change. It plays a critical role in determining and adapting crop varieties across tropical regions [1,2]. Variations in rainfall, which might be long-duration synoptic-scale rainfall and short-duration convective rainfall, are closely associated with hydrological challenges, including droughts and floods [2,3]. Extensive research has underscored the adverse effects of changes in rainfall patterns as a result of global climate change on socio-economic endeavors [4]. The consequences of climate change are not uniform, varying across different regions owing to differences in large-scale atmospheric circulation and

geographical features [5]. The repercussions are notably more acute in developing countries, where inadequate governance, compounded by various stress factors, exacerbates the situation [6,7]. Thus, a comprehensive understanding of the variability, patterns, and tendencies of rainfall within the context of an evolving climate at the regional level is crucial for evaluating the impact of climate change on agricultural outputs and water resources, as well as for devising effective mitigation strategies [8,9].

The March–April–May (MAM) season in East Africa (EA) is characterized as a major rainy season, essential for agriculture and water resources. During these months, the region experiences significant rainfall, which is critical for planting crops, replenishing water bodies, and sustaining natural ecosystems [10,11]. The precipitation patterns during MAM are vital for the livelihoods of millions, impacting food security, economic activities, and environmental health [12]. However, variability in rainfall during this season can lead to challenges such as droughts or floods, affecting communities and agriculture [13].

Rwanda, a landlocked country located in the heart of Africa, specifically EA, is predominantly agricultural, with a significant portion of its population depending on rain-fed farming for subsistence [14]. The seasonal rainfall patterns, particularly during the critical MAM season, play a pivotal role in determining the agricultural productivity and water resources management of the country [15]. This period, known as the long rains season, is crucial for the main cropping season in Rwanda [16]. However, the region has been experiencing noticeable changes and variability in rainfall patterns over recent decades, which have significant implications for food security, water resources, and disaster management [17].

The understanding of historical trends and variability in rainfall patterns is fundamental for effective agricultural planning, water resources management, and adaptation strategies to climate change. Despite the critical importance of this season for Rwanda's agriculture and hydrology, there have been limited comprehensive studies that investigate the long-term trends and variability of rainfall during the MAM season across different climatological zones of Rwanda [18]. The interannual and decadal variability of these rainfall patterns, alongside the potential drivers behind these changes, remains poorly understood [18].

Previous studies have focused on broader climatological analyses within the East African region, often overlooking the localized impacts and specificities of rainfall variability in Rwanda [19–21]. These studies have highlighted the influence of global climatic drivers, such as the El Niño Southern Oscillation (ENSO) and the Indian Ocean Dipole (IOD), on the East African short and long rains [22,23]. However, the extent to which these drivers affect the MAM rainfall season in Rwanda and the local variability patterns have not been adequately explored. Furthermore, the implications of such variability on agricultural productivity, water resource availability, and the overall socio-economic fabric of Rwanda remain under-investigated.

Given this context, the research that fulfills the gap in knowledge by providing a comprehensive analysis of historical trends and variability of rainfall patterns during the MAM season in Rwanda over the past few decades is very important, considering the use of array of meteorological data, statistical analyses, and climate modeling approaches to identify the temporal and spatial variability of rainfall, investigate the potential drivers behind observed trends, and assess the implication of rainfall variability on water resources and agricultural planning.

Furthermore, the objectives of this research are (1) to analyze historical rainfall trends during the MAM season in Rwanda over the last four decades, (2) to assess the spatial and temporal variability of MAM season rainfall across Rwanda, (3) to investigate the influence of global climatic drivers on MAM season rainfall in Rwanda, and (4) to evaluate various statistical methods to identify trends and anomalies in rainfall in Rwanda. By investigating these aspects, the study seeks to contribute to the body of knowledge on climate variability in Rwanda, offering insights that could inform policymakers, stakeholders,

and communities about adaptive strategies and resilience building in the face of changing rainfall patterns.

2. Data and Methods

2.1. Study Area

Rwanda, often referred to as the “land of a thousand hills”, is distinguished by its varied topography and remarkable geographical diversity [24]. It is a landlocked country in East Africa, 3° – 1° S and 28.75° – 31° E, that shares borders with Uganda to the north, Tanzania to the east, Burundi to the south, and the Democratic Republic of the Congo (DRC) to the west (Figure 1), and boasts a landscape that includes vast hills, plateaus, and the scenic Congo Nile basin along Lake Kivu [25]. With elevations ranging from 900 to 4507 m, Rwanda’s geography shifts from low-lying eastern regions to hillier central and southern areas, where altitudes commonly span between 1500 to 2000 m. The country covers an area of approximately 26,338 km² and is home to a population exceeding 12 million people, a majority of whom depend on agriculture as their primary means of livelihood [26].

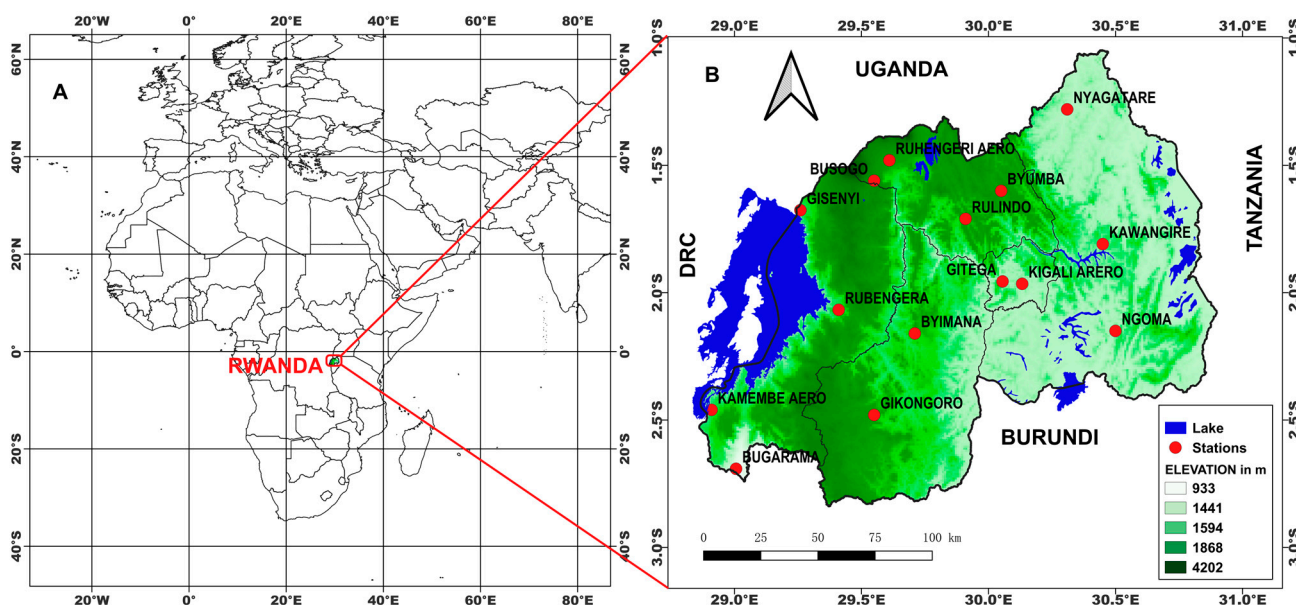


Figure 1. Study area on the map: (A) the geographical positioning of Rwanda within the East Africa region (longitude 28° – 31° E, latitude 3° – 1° S); (B) the identification and mapping of specific weather stations (red dots) across Rwanda’s landscape.

Rwanda experiences four primary climatic seasons: two rainy seasons from March to May and September to December, and two dry seasons from June to August and January to February [27]. Although the country receives abundant rainfall, averaging over 1000 mm annually in most regions, it faces irregular patterns and frequent droughts, especially in the eastern province [28]. The rainfall distribution is influenced by several factors, including the movement and intensification of the intertropical convergence zone (ITCZ), the Saint Helena high pressure system, Congo air mass, and wind movements [29]. Additionally, topography and Lake Victoria play significant roles in shaping Rwanda’s rainfall patterns [24]. During the dry season, cold and dry air masses from the Arabian Peninsula affect the climate, while moisture from the Indian Ocean influences the June to August season [30]. Additionally, the temperature variations follow a similar annual pattern to rainfall, with highs reaching up to 35° C and lows dropping to 10° C.

2.2. Data

This research incorporated multiple data types, including observed monthly rainfall figures from chosen stations, monthly reanalysis precipitation data from the Climate Hazards Group Infrared Precipitation with Station data (CHIRPS), sea surface temperatures (SSTs), and the Niño 3.4 SST anomaly index. These elements, collected on a monthly basis, were instrumental in generating seasonal analyses. An in-depth explanation of these data sources and their procurement is provided in the subsequent sections.

2.2.1. On-Site Data Collections

In this research, the Rwanda Meteorology Agency provided monthly rainfall recordings from fifteen stations over a period of thirty-nine years, spanning from 1983 to 2021. This extensive dataset was utilized to corroborate the accuracy of CHIRPS data. Additionally, a map indicating the spatial arrangement of these meteorological stations across Rwanda is depicted in Figure 1.

2.2.2. Monthly Global Precipitation Dataset from UCSB CHIRPS Version 2.0

The monthly precipitation dataset used in this study was obtained from the UCSB CHIRPS version 2.0, available through the IRI/LDEO climate data library. Covering the period from 1983 to 2021, this dataset provides detailed geographical resolution at $0.05^\circ \times 0.05^\circ$. It is a widely recognized and extensively utilized resource among researchers for its comprehensive precipitation data, which is crucial for various climate-related studies. The dataset can be accessed online at this link: <https://iridl.ldeo.columbia.edu/SOURCES/.UCSB/.CHIRPS/.v2p0/.monthly/.global/precipitation/> (accessed on 9 May 2024), offering valuable insights into historical precipitation patterns on a global scale, thereby supporting a range of environmental and climatological research projects [31,32].

2.2.3. Sea Surface Temperature

Average SST for HadISST was retrieved from <https://coastwatch.pfeg.noaa.gov/erddap/griddap/erdHadISST.html> (accessed on 9 May 2024), on a monthly basis, with a spatial resolution of $1^\circ \times 1^\circ$. The same time span (1983–2021) for the SST data was used.

2.3. Statistical Techniques

The variability of Rwanda's rainfall was examined using a range of statistical and graphical techniques including the Sen slope estimator, the Mann–Kendall trend test, correlation analysis, root mean square error (RMSE), bias, and standardized rainfall anomaly. Additionally, the empirical orthogonal functions (EOF) analysis, a statistical method used to identify the major modes of variability within a dataset and to reduce its dimensionality, was employed to examine the rainfall patterns during Rwanda's MAM season.

2.3.1. Standardized Abnormality

The rainfall anomaly was evaluated by standardizing the rainfall time series data between -1 and 1 , where plus one denotes rainy years and less than one represents anomalously dry years. Z , the standardized anomaly, may be estimated as follows:

$$Z = \frac{x - \bar{x}}{s_x} \quad (1)$$

where x denotes the recorded rainfall amounts, and \bar{x} along with s_x correspond to the rainfall's average and standard deviation, respectively.

2.3.2. Mann–Kendall (MK) Analysis

Mann (1945) and Kendall (1975) describe MK as a nonparametric statistical test used in climatological and hydrological trend analysis. This test is regarded as being very strong since it may tolerate the abrupt discontinuities brought on by an uneven time succession [33]. It is also extensively used for rainfall trend analysis since it does not need any additional assumptions about the distribution of data [34]. The MK was carried out in this research at a significant level of 0.05. For $\alpha < 0.05$, the null hypothesis, which expresses the trend's absence, is rejected. The formula for MK test statistics (S) is written as follows:

$$S = \sum_{i=1}^{n-1} \sum_{j=i+1}^n \text{sgn}(x_j - x_i) \tag{2}$$

where observations within the annual time series are specified and represented by i and j (with $j > i$), n signifies the analysis period, and the sgn function of the difference between x_j and x_i is determined as follows:

$$\text{sgn}(x_j - x_i) = \begin{cases} 1, & \text{if } x_i - x_j > 0, \\ 0, & \text{if } x_i - x_j = 0, \\ -1 & \text{if } x_i - x_j < 0. \end{cases} \tag{3}$$

when the average of the dataset is zero, the variance of S may be found using the following formula:

$$S_v = \sigma_s^2 = \frac{n(n-1)(2n+5) - \sum_{k=1}^m t_k(t_k-L)(2t_k+5)}{18} \tag{4}$$

where the amount of data in the tied group, p , is represented by t_p , the data size is represented by n , and the tied groups are denoted by q . Z statistical analysis is used to determine the trend significance.

$$z = \begin{cases} \frac{s-1}{\sigma_s} & \text{if } s > 0, \\ 0, & \text{if } s = 0 \\ \frac{s+1}{\sigma_s} & \text{if } s < 0 \end{cases} \tag{5}$$

If the measured value exceeds the tabularized α -value, then positive (negative) values of Z indicate an increasing (decreasing) trend. An effective method for identifying change points, the start of a substantial trend, and sudden changes in a series is the sequential MK test [35]. In case the intersection happens outside of the computed α -value of 1.96, an unanticipated shift at that moment is acknowledged [36]. The study used a 95% confidence level, or $\alpha = 0.05$, to evaluate the significant trend, with ± 1.96 -tabulated values serving as the equivalent.

3. Results

3.1. Evaluation of CHIRPS Dataset with Station Data

In this study, the evaluation of the CHIRPS dataset was performed by assessing the correlation between the CHIRPS data and ground station data over the entire period covered by this research. In this context, the comparison between the CHIRPS dataset and station data in capturing rainfall patterns during the MAM season in Rwanda reveals a high degree of accuracy, as evidenced by a correlation coefficient of 0.89, an RMSE of 12 in the context of rainfall amounts ranging from 0 to 300 mm, and a coefficient of determination (R^2) of 0.77, as shown in Figure 2A. These metrics collectively indicate that the CHIRPS dataset closely mirrors the actual rainfall measurements recorded at ground stations across Rwanda, capturing the wide variance in rainfall with a high level of precision. The strong positive correlation suggests that the CHIRPS dataset effectively replicates the trends and fluctuations in rainfall observed during this critical agricultural season as was previously reported [36,37]. The RMSE, when considered against the backdrop of the broad range of rainfall amounts, points to a relatively minor average deviation from the station data,

underscoring the dataset’s reliability for practical applications. Moreover, the high R^2 value indicates that the CHIRPS dataset can account for the vast majority of the variance in rainfall patterns, making it an invaluable tool for climatological studies, agricultural planning, and water resource management in Rwanda, and this result concurs with the previous research over the country [38,39]. This comparison not only highlights the potential of satellite-derived datasets like CHIRPS in enhancing our understanding of climate dynamics, but also underscores their importance in supporting decision-making processes in regions prone to climate variability.

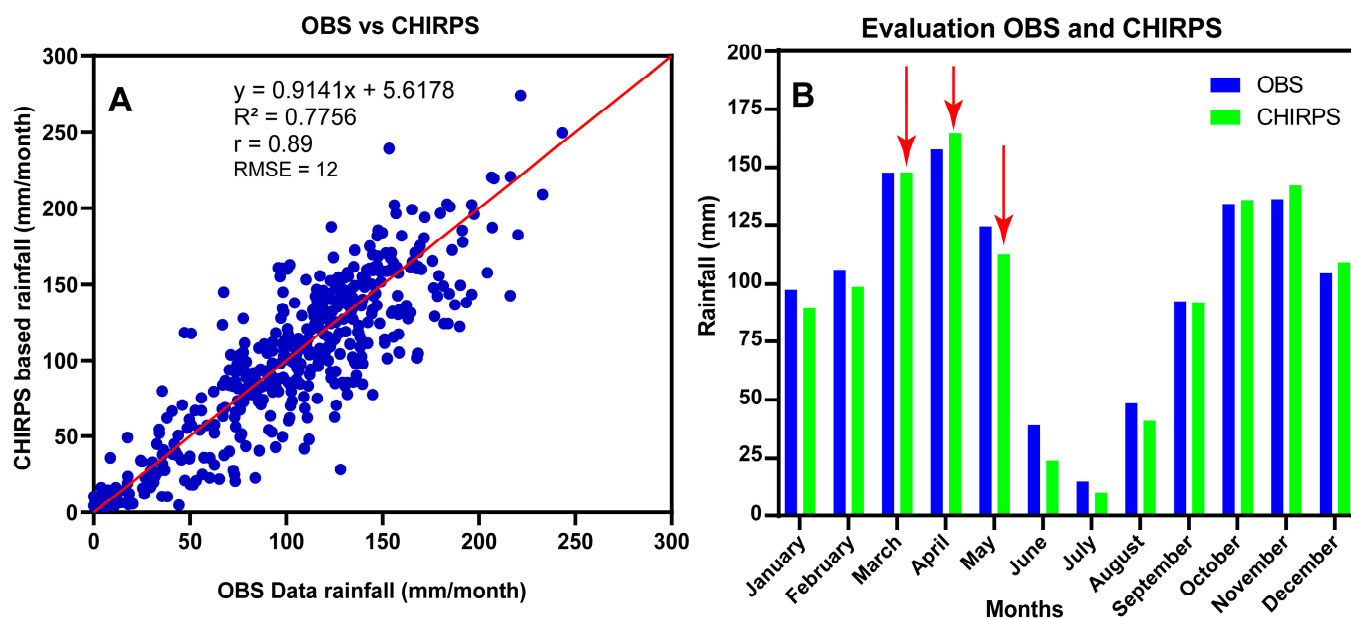


Figure 2. Evaluation of observation with CHIRPS monthly mean data: (A) indicates correlation between observation data from stations and the red line represents the regression between CHIRPS and observed rainfall. (B) shows mean annual rainfall cycle (mm) over Rwanda for observation data (blue) and CHIRPS data (green) from the period 1983–2021. The red arrows indicate the season being studied.

In the evaluation of Rwanda’s mean annual rainfall cycle, focusing on the distinct, locally named, “Long rains” (MAM) and “Short rains” (SOND) seasons [40], the comparative analysis of the CHIRPS dataset with ground station data plays a pivotal role in enhancing our understanding of the nation’s rainfall dynamics. This analysis is critical for accurately delineating the seasonal patterns, particularly noting the rainfall peaks in April for the long rains and in October for the short rains, as shown in Figure 2B. The precision of the CHIRPS dataset in mirroring the observed data from ground stations underscores its utility in capturing the complex variability and intensity of rainfall across different parts of Rwanda. Such accuracy ensures that the specific characteristics of the rainfall peaks, which are vital to understanding the climatic and environmental landscape of the region, are well represented, as was previous reported [41,42]. The efficacy of the CHIRPS dataset extends beyond mere numerical alignment; it facilitates a nuanced understanding of Rwanda’s climatic patterns, enabling researchers to dissect the seasonal fluctuations with a high degree of confidence. This precise replication of ground truth data highlights the dataset’s value in climatological research, providing a reliable basis for studies focused on temporal and spatial rainfall variations [10,11]. The ability of CHIRPS to accurately capture these critical periods of rainfall intensity is essential for a wide array of environmental assessments and policy-making processes. It allows for a more informed exploration of the climatic trends that define Rwanda, offering insights that are crucial for addressing the environmental and climatic challenges faced by the region [14].

3.2. Climatology Spatial Distribution of Rainfall over Rwanda

The investigation into the climatology and spatial distribution of rainfall over Rwanda during the MAM seasons of 1983–2021 reveals rainfall patterns that shed light on the country's hydrological dynamics (Figure 3). The quantity of seasonal rainfall within the country varies each year between 80 and 220 mm for MAM (Figure 3A). Additionally, the observed annual rainfall variations, ranging from 250 mm to 600 mm, highlight the heterogeneity of precipitation across different regions of Rwanda (Figure 3B). Particularly notable is the concentration of maximum rainfall amounts in the southwest and northwest, contrasting sharply with the lower annual rainfall observed in the eastern part of the country, and these findings concur with previous studies [43,44]. This spatial variability in rainfall distribution highlights the influence of geographical features such as mountains and elevation gradients, which can significantly impact precipitation patterns [45,46]. Moreover, the moderate levels of rainfall ranging from 50 to 350 mm observed in the central part of Rwanda suggest a transitional zone between the more arid eastern regions and the wetter western areas. The lowest rainfall amounts recorded during the MAM season in the eastern part of the country further accentuate the disparities in precipitation distribution [46]. The observed southwest to northeast slant in rainfall distribution implies a gradient that may be influenced by regional climatic drivers such as prevailing wind patterns and topographical features [42].

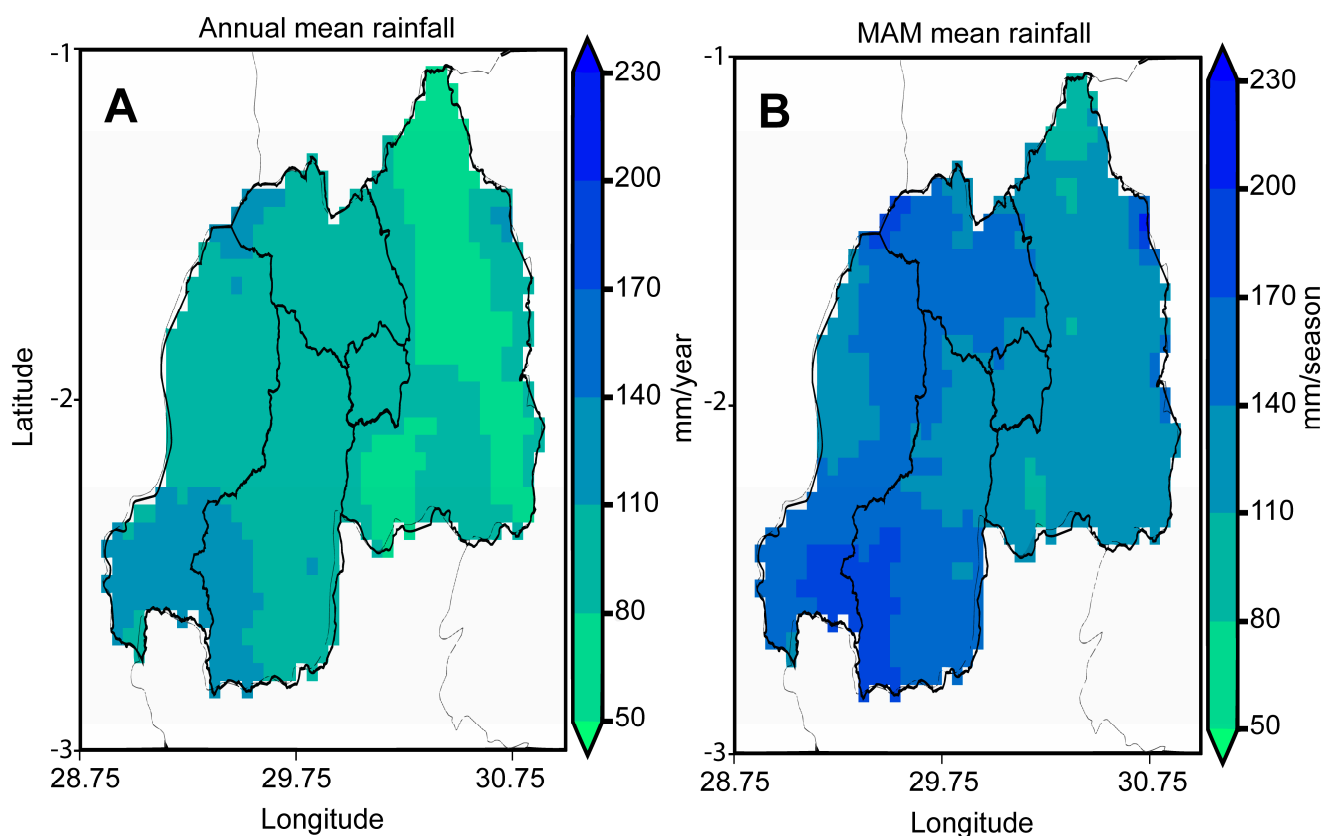


Figure 3. Climatology spatial distribution of (A) annual mean rainfall (mm/year) and (B) MAM seasonal mean rainfall (mm/season) over Rwanda 1983–2021.

Figure 4 provides a comprehensive depiction of the spatial distribution of CHIRPS monthly rainfall (mm) across Rwanda, offering valuable insights into the seasonal patterns and geographical variations in precipitation. The highest rainfall amounts are concentrated in the southwestern region of the country, particularly in April and November. This aligns with the typical seasonal rainfall distribution observed in many tropical regions, where April often marks the onset of the rainy season and November represents a secondary peak

in precipitation [40,47]. Conversely, the months of June, July, and August emerge as the driest months across Rwanda, exhibiting lighter shades on the map indicative of lower rainfall amounts during these periods. Additionally, the spatial distribution of rainfall in March, April, and May, followed by October, November, and December, showcases a clear pattern of seasonal variability across Rwanda, with these months consistently experiencing the highest levels of precipitation [48].

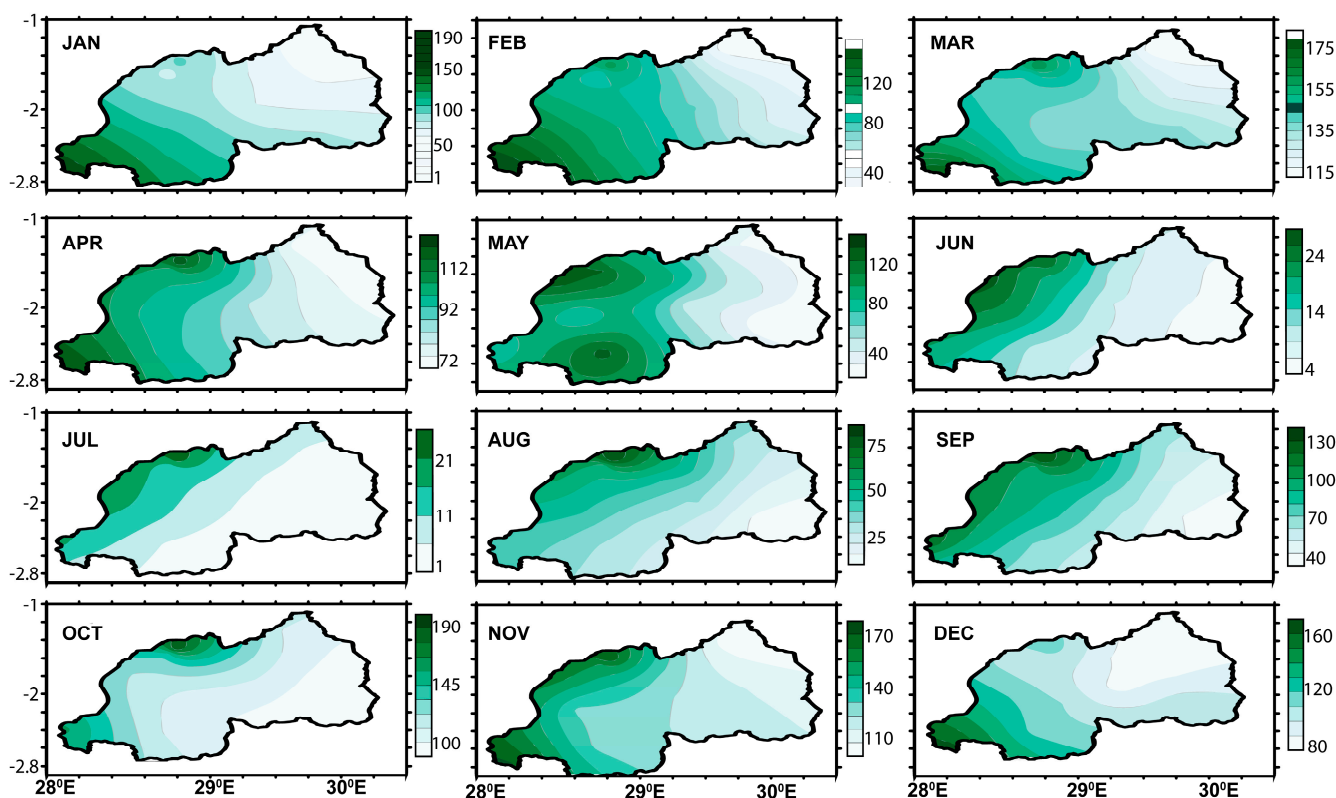


Figure 4. The distribution pattern of monthly rainfall (mm) climatology across Rwanda spanning from 1983 to 2021.

3.3. Spatial Patterns of Mann–Kendall and Sen’s Slope across the Study Area

The rainfall trends in Rwanda from 1983 to 2021 were analyzed using the Mann–Kendall trend test, examining annual and seasonal changes, including the crucial MAM period. This method effectively identifies trends in time series data, offering insights into Rwanda’s rainfall dynamics without requiring normal data distribution, crucial for its agriculture and hydrology. The analysis of rainfall trends unveiled a complex pattern of variability, with both increases and decreases observed over the study period. This intricate landscape is effectively illustrated in Figure 5, where blue and dark red hues denote areas of declining and rising rainfall, respectively, with significant trends at a 95% confidence level highlighted by black dots (Figure 5). This statistical validation provides a reliable basis for distinguishing actual changes from mere random fluctuations [48,49]. The study particularly highlights the southwestern region of Rwanda as a critical area of concern, exhibiting a significant decrease in rainfall on both the annual and the MAM seasonal scales.

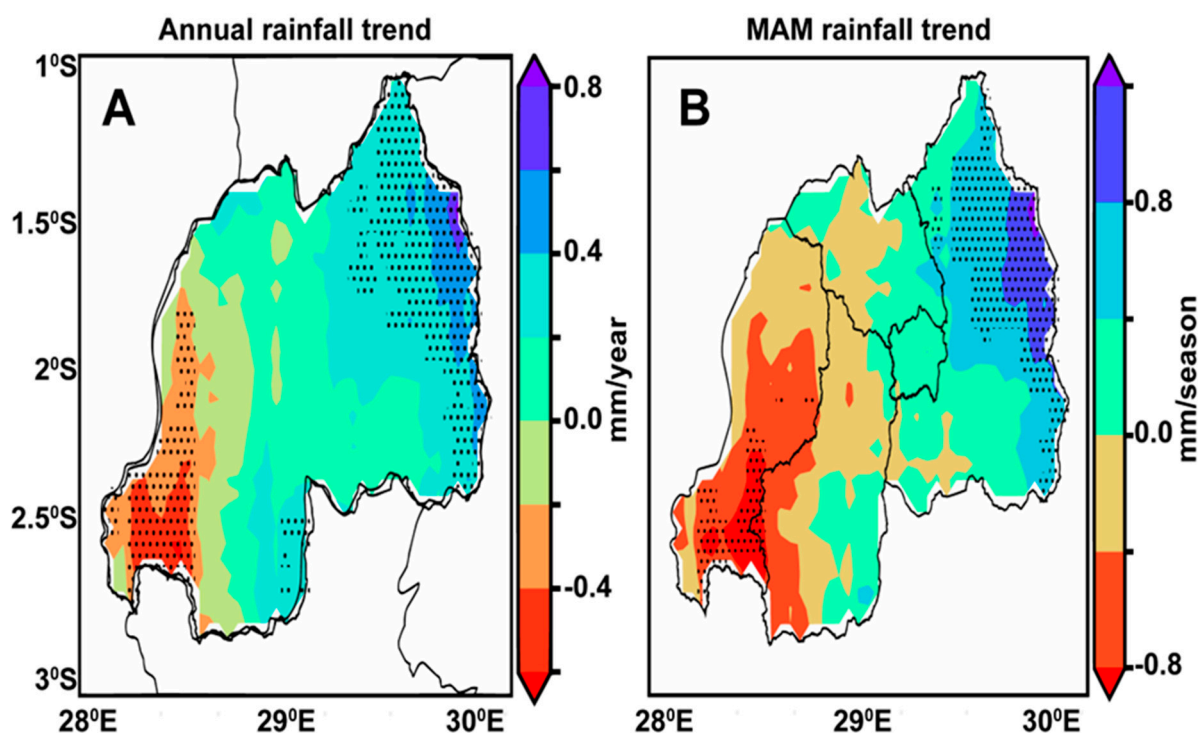


Figure 5. Geospatial trends in annual (A) and MAM seasonal (B) precipitation across Rwanda from 1983 to 2021, with significant trends in specific regions denoted by dots at a 95% confidence level.

The mixed trends, reflecting both positive and negative changes, underscore the complexity of climate variability and its influence on rainfall distribution, highlighting the importance of localized studies for revealing specific regional patterns amidst broader global shifts [46,49]. Through the Mann–Kendall test and Sen’s slope analysis, the research provides a detailed insight into the spatial dynamics of rainfall trends across Rwanda, especially emphasizing the need for focused attention on the southwestern parts to understand the implications for ecosystems and human activities reliant on consistent rainfall.

Additionally, the Mann–Kendall test and Sen’s slope analysis reveal a nuanced spatial pattern of rainfall changes across Rwanda, highlighting variability that escapes a uniform trend across all months. Specifically, the analysis indicates no significant change in rainfall for most months, with the exception of March, April, July, October, and November (Figure 6), and these findings concur with the previous studies [49,50]. In March, there is a noteworthy increasing trend in rainfall in the northeast, southeast, central, and northwest regions, compared with a decreasing trend in the southwest. April further highlights this variability, with an increasing trend observed in the east, contrasted by decreases in the west, south, and central areas. As previously reported, the pattern shifts in July, where significant decreases are noted in the west and southeast, while October’s data reveal an increase in the east but a decrease in the southwest.

Moreover, November brings an increase in rainfall to the northwest, with the southwest continuing to experience a downward trend [43,48]. These findings underscore the complex interplay of climatic factors influencing rainfall distribution in Rwanda, emphasizing region-specific trends that manifest distinct patterns of change within the country’s diverse climatic zones. This spatial and temporal variability in rainfall trends points to the intricate dynamics of climate change impacts, necessitating targeted adaptation and mitigation strategies to address the specific needs and vulnerabilities of each region.

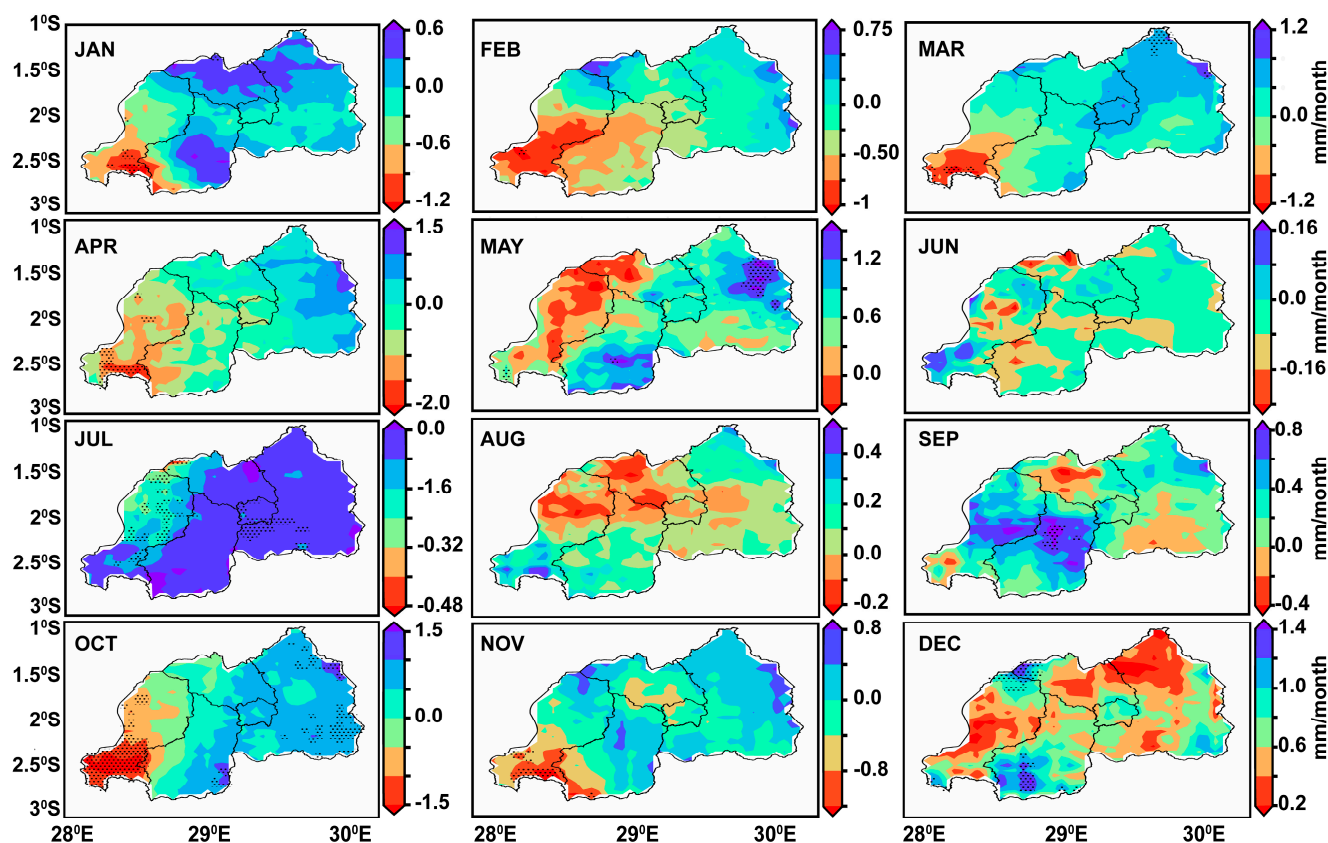


Figure 6. Distribution of monthly rainfall trends across Rwanda on a spatial basis, with black-dotted areas highlighting statistically significant differences at the 95% confidence threshold.

3.4. Temporal Variations in Rainfall

This section presents an in-depth analysis of the changing patterns of rainfall in Rwanda over a 36-year period, from 1983 to 2021, as shown in Figure 7. This comprehensive study highlights the significant inter-annual variability in rainfall, on both an annual and seasonal scale, specifically during the MAM season, which is critical for the region's agricultural practices. The findings reveal a distinct classification of years based on standardized rainfall anomalies, identifying eight particularly wet years (1987, 1988, 2001, 2006, 2010, 2011, 2012, 2018) and eight markedly dry years (1984, 1993, 1999, 2000, 2003, 2005, 2008, 2014) on an annual basis (Figure 7A). Moreover, the analysis extends to seasonal variations, where eight years were exceptionally wet (1987, 1988, 2006, 2012, 2016, 2018) during the MAM season, contrasted against six years that experienced significantly lower precipitation (1984, 1996, 2000, 2008, 2014, 2017), as shown in Figure 7B. Notably, the year 2018 stood out as an anomaly, being extraordinarily wet, contrasting sharply with 2017, which was marked by minimal rainfall, and these results concur with the previous findings across the country [29,40,51]. This detailed exploration into the temporal dynamics of rainfall in Rwanda not only highlights the region's vulnerability to climatic variability but also emphasizes the critical need for adaptive strategies in water resource management and agricultural planning to mitigate the impacts of these fluctuating weather patterns.

Figure 8 provides a comprehensive overview of the variation in rainfall patterns in Rwanda from 1983 to 2021, covering a detailed month-by-month analysis from January to December. This extensive period of observation uncovers significant insights into the climatic variability experienced across the country, highlighting both wet and dry years in terms of monthly rainfall. The analysis, focused on 15 meteorological stations, documented varying trends of precipitation, highlighting the spatial diversity in climatic responses across the region. A handful of stations such as Rulindo, Gisenyi Aero, Byimana,

Busogo, and Gikongoro present stable precipitation patterns, devoid of significant long-term changes, which is a rarity in the context of broader climatic fluctuations [28,52,53]. Conversely, stations like Bugarama and Nyagatare signify the extremes of these temporal variations, with Bugarama experiencing a marked decline in rainfall, whereas Nyagatare sees a noticeable uptick. These contrasting trends highlight the localized and heterogeneous nature of rainfall variability within Rwanda, emphasizing the need for region-specific climatological studies [42,52,54,55].

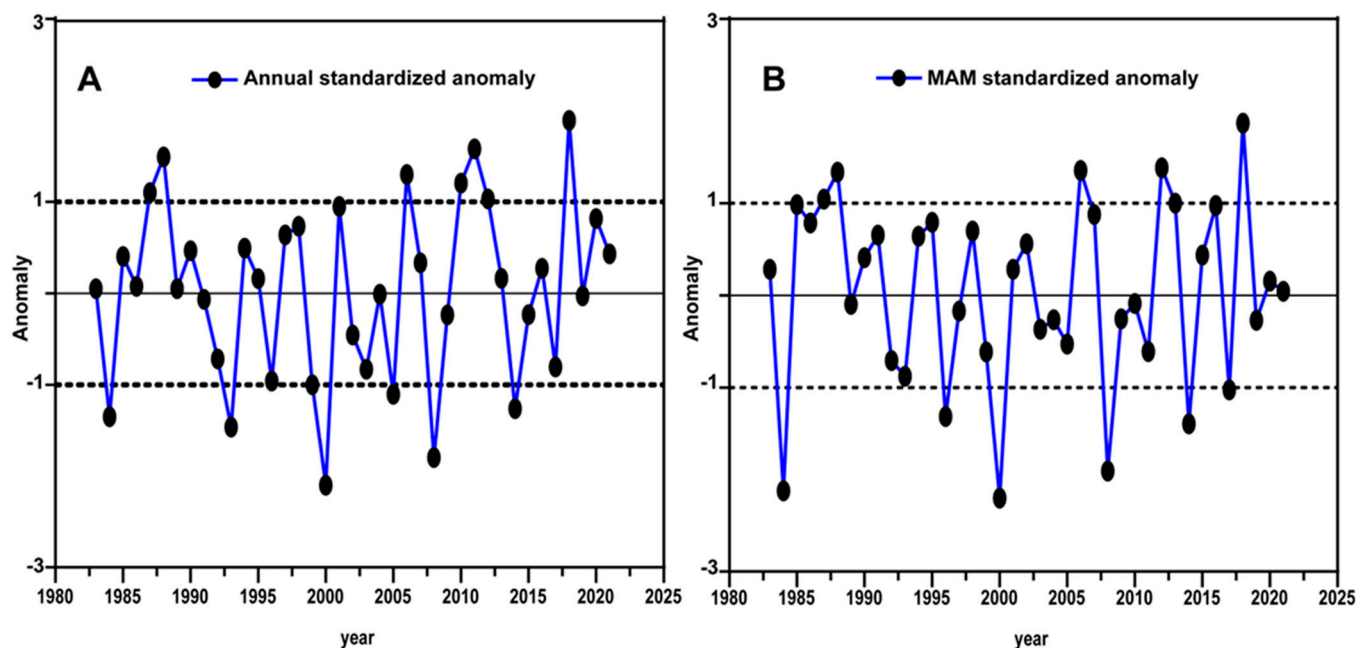


Figure 7. The inter-annual variability of rainfall at annual and seasonal (MAM) scale over Rwanda for the period 1983–2021.

3.5. Analysis of Empirical Orthogonal Function (EOF)

The analysis of EOF applied to rainfall variability during the MAM season over Rwanda from 1983 to 2021 reveals a detailed understanding of spatial and temporal rainfall patterns across the region (Figure 9). Utilizing EOF1, EOF2, and EOF3 modes to dissect the dataset, it becomes evident that these modes encapsulate a significant portion of the total variance in seasonal rainfall, with EOF1 accounting for 51.19%, EOF2 for 22.52%, and EOF3 for 8.41%. This hierarchical decomposition of rainfall variability stresses the dominant influence of EOF1, which is characterized by a distinctive west–east precipitation gradient across the country as shown in previous studies [56,57]. Specifically, EOF1 delineates a pattern of weak to strong positive loadings in the western, northern, and southern sectors, contrasted by general negative loadings across the eastern regions. This spatial configuration suggests a pronounced dipole effect within the country’s climatic system, likely driven by complex interactions between topographical features and atmospheric circulation dynamics [58,59].

The EOF1 mode, in particular, highlights a predominant negative anomaly over much of Rwanda, except for localized areas of positive factor loading in the western corridor, alongside significant positive anomalies in the northeast and southwest. Such distribution indicates that EOF1 captures the primary mode of seasonal rainfall variability, potentially linked to large-scale atmospheric phenomena such as the East African monsoon system and its modulation by the intertropical convergence zone (ITCZ) [59,60]. The presence of positive loadings in the west and the stark contrasts observed across the EOF patterns could be indicative of orographic lifting effects, where elevated terrain in the west enhances convective activity, leading to increased precipitation, while eastern regions experience

rain shadow effects. Furthermore, the variance contributions of EOF2 and EOF3, though lesser than EOF1, are critical in understanding secondary and tertiary patterns of rainfall variability, which may be influenced by other meteorological factors such as regional temperature gradients, variations in sea surface temperatures, and teleconnections with global climate indices [61]. The delineation of these EOF modes offers invaluable insights into the climatological processes driving seasonal rainfall patterns in Rwanda, particularly in identifying areas prone to extreme rainfall events during the MAM season.

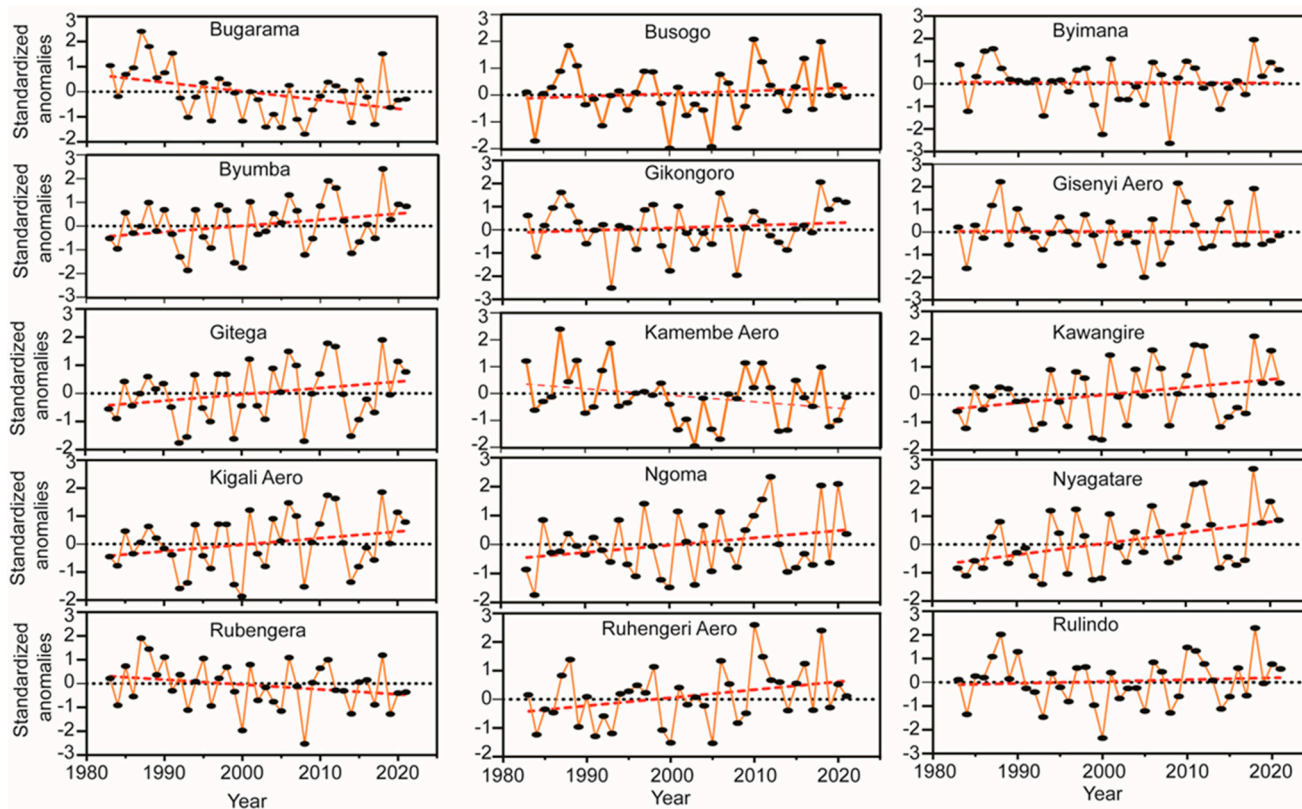


Figure 8. Trend analysis for inter-annual rainfall variability of 15 stations from 1983 to 2021.

The first principal component (PC1) effectively captures the temporal variability of rainfall, identifying distinct wet and dry years based on a standardized threshold, with +1 signifying wet years (1985, 1987, 1988, 2012, and 2018) and −1 indicating dry years (1984, 1996, 2000, 2008, 2014, and 2017). This divergence underlines the robustness of PC1 in discerning anomalous hydroclimatic conditions over the study period [62]. On the spatial front, EOF2 elucidates the geographical distribution of rainfall anomalies, revealing a pattern of positive loading in the western regions contrasted by negative loadings in other parts, indicative of a noticeable west–east moisture gradient [42]. PC2, associated with EOF2, further segments the temporal axis into six wet years (1986, 1996, 2002, 2006, 2016, 2017, and 2018) and five dry years (1987, 1988, 1990, 2000, and 2010), reinforcing the dynamic interplay between spatial and temporal variability in rainfall. Remarkably, EOF2 accounts for 22.52% of the total variance, signifying its substantial contribution to understanding the overall variability. The delineation of a unimodal pattern in eastern and central areas with significant positive loading by EOF2, alongside the minimal variability in rainfall in the northern and southern regions as indicated by the smallest positive loadings, suggests a nuanced understanding of regional precipitation dynamics [58,63]. Additionally, the analysis, however, revealed that the contributions of EOF3 and its associated PC3 to understanding rainfall variability were negligible. This minimal influence suggests that while the first two EOFs capture the primary modes of variability effectively, capturing substantial portions of the variance, the third EOF does not significantly contribute to explaining additional variability in the dataset [59,63,64].

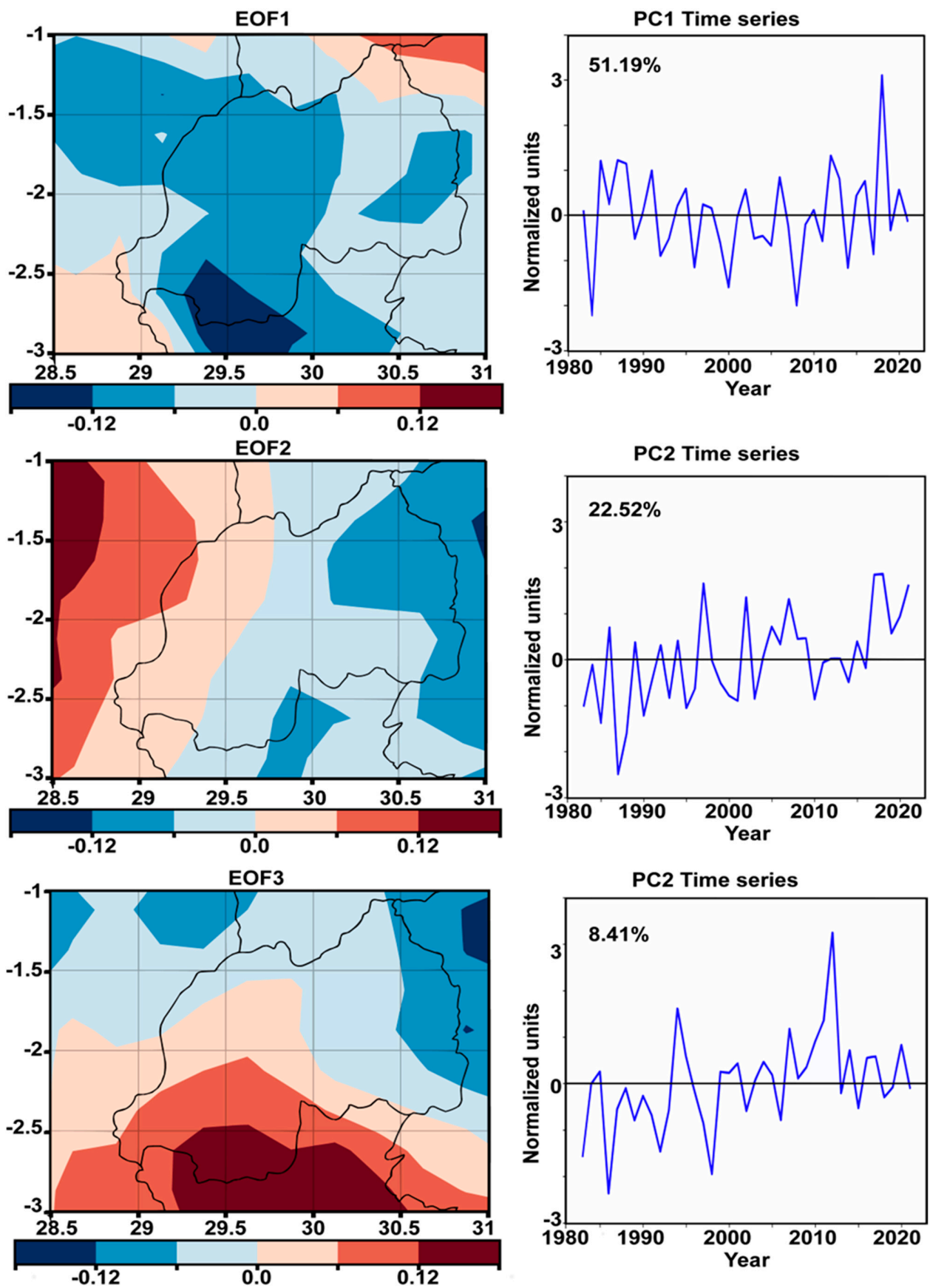


Figure 9. The spatial variability of EOF1, EOF2, and EOF3, along with the time series of principal components (PCs) for the MAM season from 1983 to 2023.

3.6. Correlation between SSTs and Rainfall Patterns, Focusing on the MAM Period

The correlation between SSTs and rainfall patterns, particularly during the MAM period, presents a complex but discernible pattern that significantly affects regional climates and, more specifically, rainfall distribution in Rwanda during the period 1983–2021. In Figure 10, the correlation of rainfall with global SSTs at a MAM seasonal scale is shown, which offers insight into the intricate relationship between oceanic temperatures and precipitation patterns. The use of blue and brown shades to represent negative and positive correlations, respectively, helps to investigate and analyze the spatial correlation patterns across different parts of the globe.

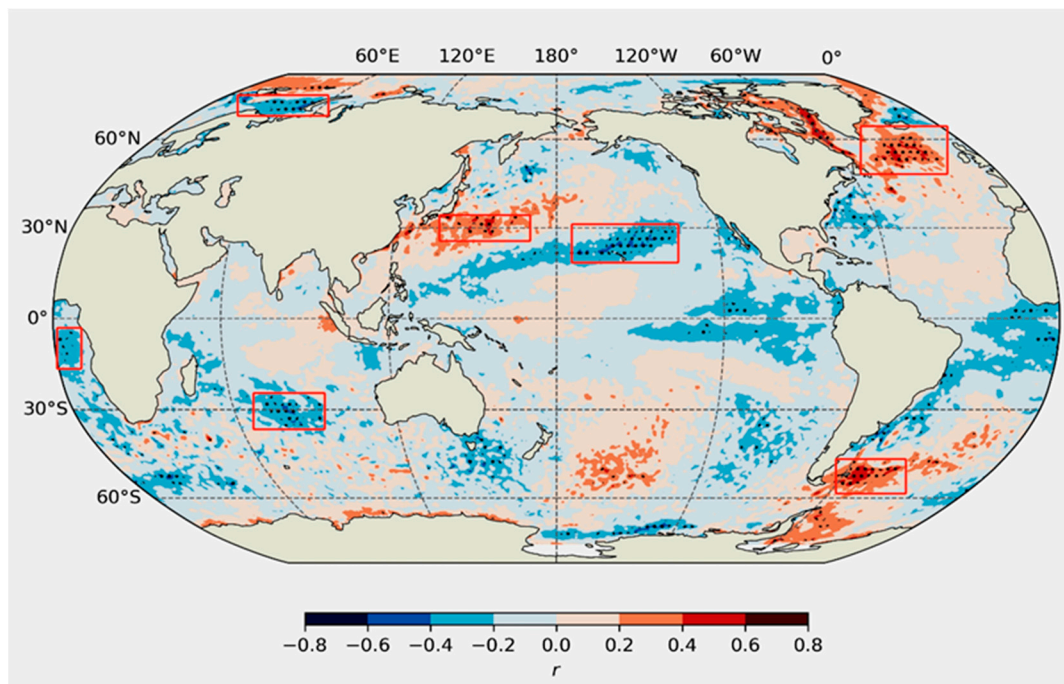


Figure 10. Spatial relationship of average MAM rainfall anomaly with global SST anomaly from 1983 to 2021.

The spatial correlation patterns observed during the MAM rainy seasons with global SSTs range between -0.8 and 0.8 , as shown in Figure 10. This indicates a varying degree of influence that different ocean basins exert on rainfall over Rwanda during this specific period, as previously reported [65,66]. Notably, the Indian Ocean exhibits a lesser impact on MAM season rainfall in Rwanda.

This observation is significant because it suggests that while the Indian Ocean is a critical driver of climate variability in many parts of East Africa, its direct influence on rainfall during the MAM season in Rwanda is relatively subdued [67,68]. The positive phase of the IOD, commonly referred to as the positive dipole, correlates with increased precipitation over EA in general [42]. This suggests that during years when the western Indian Ocean is warmer relative to the eastern part, there is a tendency for more rainfall in the region [52,69]. Conversely, the negative phase of the IOD, characterized by cooler surface waters in the western Indian Ocean, is associated with reduced rainfall over Rwanda [58]. This inverse relationship highlights the IOD's significant role in modulating rainfall patterns over East Africa, including Rwanda, during the MAM season.

Additionally, it was previously reported that there is a strong positive correlation between MAM rainfall in Rwanda and SSTs in the South Atlantic Ocean [70–72]. This relationship highlights the broader climatic relationship between the Atlantic Ocean and East African rainfall patterns including those of Rwanda. The positive correlation suggests that warmer surface temperatures in the South Atlantic Ocean can enhance MAM rainfall

in Rwanda, a relationship that is crucial for understanding and predicting seasonal rainfall variability in the region [25,65]. Furthermore, the analysis indicates a high negative correlation between MAM rainfall in Rwanda and the South African ridge. This negative correlation implies that atmospheric conditions associated with the South African ridge, such as high-pressure systems, might inhibit moisture flow and rainfall over Rwanda during the MAM season [40,65,68,70].

3.7. Relationship between Geopotential and Rainfall at MAM Season

The relationship between geopotential heights (GH) at different atmospheric levels (specifically 500 hPa and 850 hPa) and rainfall during the MAM season in Rwanda over the period of 1983–2021 is a complex interplay of atmospheric dynamics and moisture transport mechanisms (Figure 11). This relationship is further influenced by macro-scale pressure systems developed in the Indian and Atlantic Oceans, as well as monsoon flows, which collectively impact the seasonal and annual rainfall variations not only in Rwanda but also in the broader East African region.

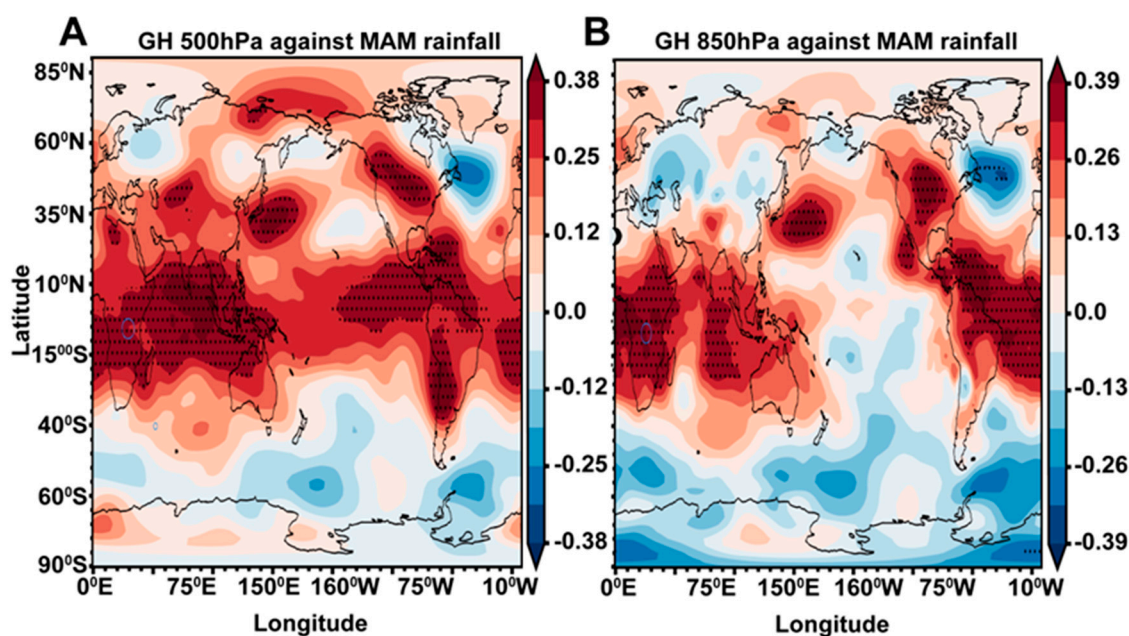


Figure 11. The correlation between geopotential height at (A) 500 hpa upper level and (B) 850 hpa low-level from 1983 to 2021.

At the 500 hPa level, the GH is a crucial parameter for understanding mid-tropospheric circulation patterns. These patterns are instrumental in steering air masses and associated moisture towards or away from specific regions, such as Rwanda, thereby exerting a significant influence on local rainfall patterns [62,66]. The mid-troposphere is characterized by the movement of large-scale weather systems, which can either promote or inhibit the conditions necessary for precipitation [73]. For instance, the presence of strong gradients in geopotential height at this level can induce ascending air masses, a process that is conducive to cloud formation and, subsequently, rainfall. This vertical motion in the atmosphere is a key component in the development of precipitation, as it facilitates the lifting of moist air, cooling, and condensation to form cloud droplets [74]. The interaction between surface low-pressure systems and upper-level atmospheric patterns can further enhance these processes, leading to significant rainfall events. The correlation between geopotential height at the 500 hPa level and rainfall in Rwanda during the MAM season has been quantitatively established, with a positive correlation ranging from +0.25 to +0.38 at a 95% confidence level, as shown in Figure 11A.

Conversely, the 850 hPa level is closer to the Earth's surface and plays a pivotal role in the low-level transport of moisture [71,75]. GHs at this atmospheric level are indicative of the presence and characteristics of air masses; low heights often signal the presence of moist air masses, while high heights are indicative of drier conditions [66,67,73]. The distribution and movement of these air masses are critical in determining the moisture availability for precipitation over Rwanda. The low-level circulation patterns are sensitive to local geographical features, including topography and land surface conditions. Rwanda's varied landscape, marked by mountains and valleys, exerts a profound influence on the flow of air and moisture at this level, modifying rainfall patterns across different regions of the country. The significant positive correlation between geopotential height at the 850 hPa level and rainfall during the MAM season, approximately equal to +0.38 with a 95% confidence level as shown in Figure 11B, highlights the importance of understanding the dynamics at this level to predict rainfall patterns.

The analysis of GH at both 500 hPa and 850 hPa levels reveals the intricate mechanisms through which atmospheric circulation patterns influence rainfall in Rwanda, especially during the critical MAM season. These findings highlight the need for comprehensive atmospheric monitoring and modeling to predict rainfall patterns accurately. Understanding the relationship between GH and rainfall is vital for developing effective water resource management and agricultural planning strategies in Rwanda and the wider East African region, where rainfall variability has significant socio-economic impacts. The combined effects of mid-tropospheric circulation patterns and low-level moisture transport mechanisms, as influenced by large-scale pressure systems and local geographical features, underscore the complexity of predicting rainfall in this region. Future research efforts should continue to explore these dynamics, incorporating advanced atmospheric modeling techniques and long-term climate data analysis to improve the accuracy of rainfall forecasts and mitigate the impacts of climate variability on vulnerable communities.

4. Conclusions

This study rigorously evaluates the CHIRPS satellite dataset against terrestrial hydrometeorological measurements, illustrating its efficacy in accurately capturing Rwanda's precipitation dynamics across variable temporal and spatial domains. CHIRPS' high fidelity in reflecting seasonal pluvial patterns, specifically the "Long rains" and "Short rains," along with its detailed depiction of Rwanda's complex rainfall distribution, highlights its critical role in hydroclimate studies. The integration of statistical analyses, including the Mann–Kendall trend test and Sen's slope estimator, reveals nuanced temporal and spatial rainfall trends, highlighting the pronounced influence of climatic variability on regional precipitation regimes. Further, the study's application of EOFs dissects the primary modes of rainfall variability, emphasizing the significant impact of atmospheric and oceanic interactions on Rwanda's rainfall, particularly the role of SSTs and GH. The correlation between SSTs in the Indian and South Atlantic Oceans and Rwanda's MAM season precipitation patterns elucidates the complex global-to-local climatological linkages influencing rainfall distribution. These findings advocate for the development of targeted adaptation and mitigation strategies to address the impacts of climatic fluctuations, reinforcing the need for advanced analytical methodologies and datasets in enhancing predictive accuracy and hydrological resilience in the face of climate change.

Author Contributions: C.U.: investigation, formal analysis, writing—original draft, validation, writing—review and editing. L.J.: conceptualization, methodology, resources, formal analysis, writing—original draft, validation, writing—review and editing. T.H.: validation, writing—review and editing. A.A.B.: writing—review and editing. All authors have read and agreed to the published version of the manuscript.

Funding: This work was supported by National Natural Science Foundation of China (42288101), Laoshan Laboratory (No. LSKJ202202600), and Shandong Natural Science Foundation Project (ZR2019ZD12).

Institutional Review Board Statement: Not applicable.

Informed Consent Statement: Not applicable.

Data Availability Statement: Observation Data: Rwanda Meteorology agency (ENACTs dataset), NOAA/NCEI: Global SST& IOD, ECWMF: CHIRPS data, ERA5: Geopotential height (<https://psl.noaa.gov/data/gridded/data.ncep.reanalysis.html>, accessed on 20 March 2024).

Acknowledgments: The authors extend their profound gratitude to the Ocean University of China (OUC) for fostering an environment conducive to research, providing us with the necessary resources and opportunities to pursue our investigations. Our special appreciation is reserved for the Rwanda Meteorology Agency (RMA), whose unparalleled support played a crucial role in the advancement of our research.

Conflicts of Interest: The authors hereby declare that there are no known competing financial interests or personal relationships that could have influenced the outcomes or interpretations of the work presented in this paper.

References

1. Maity, A.; Paul, D.; Lamichaney, A.; Sarkar, A.; Babbar, N.; Mandal, N.; Dutta, S.; Maity, P.P.; Chakrabarty, S.K. Climate change impacts on seed production and quality: Current knowledge, implications, and mitigation strategies. *Seed Sci. Technol.* **2023**, *51*, 65–96. [[CrossRef](#)]
2. Özdemir, E.T.; Yavuz, V.; Deniz, A.; Karan, H.; Kartal, M.; Kent, S. Squall line over Antalya: A case study of the events of 25 October 2014. *Weather* **2019**, *74*, S1–S6. [[CrossRef](#)]
3. Ansari, A.; Pranesti, A.; Telaumbanua, M.; Alam, T.; Taryono; Wulandari, R.A.; Nugroho, B.D.A.; Supriyanta. Evaluating the effect of climate change on rice production in Indonesia using multimodelling approach. *Heliyon* **2023**, *9*, e19639. [[CrossRef](#)] [[PubMed](#)]
4. Adeagbo, O.; Bamire, A.; Akinola, A.; Adeagbo, A.; Oluwole, T.; Ojedokun, O.; Ojo, T.; Kassem, H.; Emenike, C. The level of adoption of multiple climate change adaptation strategies: Evidence from smallholder maize farmers in Southwest Nigeria. *Sci. Afr.* **2023**, *22*, e01971. [[CrossRef](#)]
5. Shah, I.H.; Manzoor, M.A.; Jinhui, W.; Li, X.; Hameed, M.K.; Rehman, A.; Li, P.; Zhang, Y.; Niu, Q.; Chang, L. Comprehensive review: Effects of climate change and greenhouse gases emission relevance to environmental stress on horticultural crops and management. *J. Environ. Manag.* **2024**, *351*, 119978. [[CrossRef](#)] [[PubMed](#)]
6. Scott, D.; Hall, C.M.; Stefan, G. *Tourism and Climate Change: Impacts, Adaptation and Mitigation*; Routledge: Oxfordshire, UK, 2012; ISBN 1136462937.
7. Huang, M.-T.; Zhai, P.-M. Achieving Paris Agreement temperature goals requires carbon neutrality by middle century with far-reaching transitions in the whole society. *Adv. Clim. Chang. Res.* **2021**, *12*, 281–286. [[CrossRef](#)]
8. Nsubuga, F.W.; Rautenbach, H. Climate change and variability: A review of what is known and ought to be known for Uganda. *Int. J. Clim. Chang. Strat. Manag.* **2018**, *10*, 752–771. [[CrossRef](#)]
9. Urama, K.C.; Ozor, N. Impacts of climate change on water resources in Africa: The role of adaptation. *Afr. Technol. Policy Stud. Netw.* **2010**, *29*, 1–29.
10. Mbigi, D.; Onyango, A.O.; Mtewe, Z.F.; Kiprotich, P.; Xiao, Z. Coupled Model Intercomparison Project Phase 6 simulations of the spatial structure of rainfall variability over East Africa: Evaluation and projection. *Int. J. Climatol.* **2022**, *42*, 9865–9885. [[CrossRef](#)]
11. Nkunzimana, A.; Shuoben, B.; Guojie, W.; Alriah, M.A.A.; Sarfo, I.; Zhihui, X.; Vuguziga, F.; Ayugi, B.O. Assessment of drought events, their trend and teleconnection factors over Burundi, East Africa. *Theor. Appl. Climatol.* **2021**, *145*, 1293–1316. [[CrossRef](#)]
12. Ayugi, B.; Dike, V.; Ngoma, H.; Babaousmail, H.; Mumo, R.; Ongoma, V. Future Changes in Precipitation Extremes over East Africa Based on CMIP6 Models. *Water* **2021**, *13*, 2358. [[CrossRef](#)]
13. Funk, C.; Fink, A.H.; Harrison, L.; Segele, Z.; Endris, H.S.; Galu, G.; Korecha, D.; Nicholson, S. Frequent but Predictable Droughts in East Africa Driven by a Walker Circulation Intensification. *Earth's Futur.* **2023**, *11*, e2022EF003454. [[CrossRef](#)]
14. Muhamadi, S.; Boz, I. Factors influencing farmers' perception of sustainable agriculture: A case study of Musanze District, Rwanda. *Int. J. Sustain. Agric. Manag. Inform.* **2022**, *8*, 408–424. [[CrossRef](#)]
15. Craig, A.; Hutton, C.; Lewis, L.A.; Musa, F.B.; Sheffield, J. Linking household access to food and social capital typologies in Phalombe District, Malawi. *Sustain. Sci.* **2023**, *18*, 1721–1737. [[CrossRef](#)]
16. Islam, S.M.F.; Karim, Z. World's Demand for Food and Water: The Consequences of Climate Change. In *Desalination—Challenges and Opportunities*; IntechOpen: London, UK, 2020. [[CrossRef](#)]
17. Dube, T.; Moyo, P.; Ncube, M.; Nyathi, D. The Impact of Climate Change on Agro-Ecological Based Livelihoods in Africa: A Review. *J. Sustain. Dev.* **2016**, *9*, 256. [[CrossRef](#)]
18. Maja, M.M.; Ayano, S.F. The Impact of Population Growth on Natural Resources and Farmers' Capacity to Adapt to Climate Change in Low-Income Countries. *Earth Syst. Environ.* **2021**, *5*, 271–283. [[CrossRef](#)]

19. He, J.; Garzanti, E.; Dinis, P.; Yang, S.; Wang, H. Provenance versus weathering control on sediment composition in tropical monsoonal climate (South China)—1. Geochemistry and clay mineralogy. *Chem. Geol.* **2020**, *558*, 119860. [[CrossRef](#)]
20. Kim, Y.-H.; Min, S.-K.; Zhang, X.; Sillmann, J.; Sandstad, M. Evaluation of the CMIP6 multi-model ensemble for climate extreme indices. *Weather Clim. Extrem.* **2020**, *29*, 100269. [[CrossRef](#)]
21. Kaskaoutis, D.; Houssos, E.; Solmon, F.; Legrand, M.; Rashki, A.; Dumka, U.; Francois, P.; Gautam, R.; Singh, R. Impact of atmospheric circulation types on southwest Asian dust and Indian summer monsoon rainfall. *Atmos. Res.* **2018**, *201*, 189–205. [[CrossRef](#)]
22. Adhikari, U.; Nejadhashemi, A.P.; Woznicki, S.A. Climate change and eastern Africa: A review of impact on major crops. *Food Energy Secur.* **2015**, *4*, 110–132. [[CrossRef](#)]
23. Cawthra, H.C.; Jacobs, Z.; Wadley, L. Winds of change: Climate variability in a mild glacial on the east coast of South Africa, inferred from submerged aeolianites and the archaeological record of Sibudu. *Quat. Int.* **2022**, *638–639*, 23–36. [[CrossRef](#)]
24. Nwazelibwe, V.E.; Egbueri, J.C.; Unigwe, C.O.; Agbasi, J.C.; Ayejoto, D.A.; Abba, S.I. GIS-based landslide susceptibility mapping of Western Rwanda: An integrated artificial neural network, frequency ratio, and Shannon entropy approach. *Environ. Earth Sci.* **2023**, *82*, 439. [[CrossRef](#)]
25. Uwimbabazi, J.; Jing, Y.; Iyakaremye, V.; Ullah, I. Observed Changes in Meteorological Drought Events during 1981–2020 over Rwanda, East Africa. *Sustainability* **2022**, *14*, 1519. [[CrossRef](#)]
26. Sekiyama, M.; Matsuda, H.; Mohan, G.; Yanagisawa, A.; Sudo, N.; Amitani, Y.; Caballero, Y.; Matsuoka, T.; Imanishi, H.; Sasaki, T. Tackling Child Malnutrition by Strengthening the Linkage Between Agricultural Production, Food Security, and Nutrition in Rural Rwanda. In *Sustainability Challenges in Sub-Saharan Africa II: Insights from Eastern and Southern Africa*; Springer: Berlin/Heidelberg, Germany, 2020; pp. 3–28.
27. de Dieu Ndayisenga, J.; Mupenzi, C. Analysis of Rainfall and Temperature at Kamembe in Western Province of Rwanda. *East Afr. J. Sci.* **2020**, *10*.
28. Twahirwa, A.; Oludhe, C.; Omondi, P.; Rwanyiziri, G.; Ndakize, J.S. Assessing Variability and Trends of Rainfall and Temperature for the District of Musanze in Rwanda. *Adv. Meteorol.* **2023**, *2023*, 7177776. [[CrossRef](#)]
29. Sebaziga, J.N.; Twahirwa, A.; Kazora, J.; Rusanganwa, F.; Mbatu, M.M.; Higiyo, S.; Guhirwa, S.; Nyandwi, J.C.; Niyitegeka, J.M.V. Spatial and Temporal Analysis of Rainfall Variability and Trends for Improved Climate Risk Management in Kayanza District, Eastern Rwanda. *Adv. Meteorol.* **2023**, *2023*, 5372701. [[CrossRef](#)]
30. Mahmoud, S.H.; Gan, T.Y. Multidecadal variability in the Nile River basin hydroclimate controlled by ENSO and Indian Ocean dipole. *Sci. Total. Environ.* **2020**, *748*, 141529. [[CrossRef](#)]
31. Rivera, J.A.; Marianetti, G.; Hinrichs, S. Validation of CHIRPS precipitation dataset along the Central Andes of Argentina. *Atmos. Res.* **2018**, *213*, 437–449. [[CrossRef](#)]
32. López-Bermeo, C.; Montoya, R.D.; Caro-Lopera, F.J.; Díaz-García, J.A. Validation of the accuracy of the CHIRPS precipitation dataset at representing climate variability in a tropical mountainous region of South America. *Phys. Chem. Earth Parts A/B/C* **2022**, *127*, 103184. [[CrossRef](#)]
33. Waiswa, M. Assessment of Spatial and Temporal Characteristics of the December-February Seasonal Rains over Uganda. Ph.D. Thesis, University of Nairobi, Nairobi, Kenya, 2015.
34. Caviglioni, L. Designing Efficient Reservoir Filling Strategies Using Seasonal Drought Forecasts. Ph.D. Thesis, Politecnico di Milano, Milan, Italy, 2017.
35. Karama, A. *East African Seasonal Rainfall Prediction Using Multiple Linear Regression and Regression with ARIMA Errors Models*; Bayerische Julius-Maximilians-Universität: Würzburg, Germany, 2021; ISBN 9798426876774.
36. de Assis Paiva, D.; Sáfiadi, T. Study of tests for trend in time series. *Braz. J. Biom.* **2021**, *39*, 311–333.
37. Jamali, M.; Eslamian, S. Parametric and nonparametric methods for analyzing the trend of extreme events. In *Handbook of Hydroinformatics*; Elsevier: Amsterdam, The Netherlands, 2023; pp. 223–237.
38. Cabral Júnior, J.B.; Lucena, R.L. Analysis of precipitation using Mann-Kendall and Kruskal-Wallis non-parametric tests. *Mercator* **2020**, *19*, e19001. [[CrossRef](#)]
39. Ntawukuriryayo, E. Applicability of Satellite-Based Rainfall Estimates and Inundation Extent for Flood Modeling in the Sebeya Catchment, Rwanda. Master's Thesis, University of Twente, Enschede, The Netherlands, 2022.
40. Muthike, D.M. Evaluating Climate Resilience in Rural East Africa Using Mixed Method Experimental Studies, Remote Sensing and Machine Learning. Ph.D. Thesis, University of Colorado at Boulder, Boulder, CO, USA, 2023.
41. Kalisa, W.; Zhang, J.; Igbawua, T.; Ujoh, F.; Ebohon, O.J.; Namugize, J.N.; Yao, F. Spatio-temporal analysis of drought and return periods over the East African region using Standardized Precipitation Index from 1920 to 2016. *Agric. Water Manag.* **2020**, *237*, 106195. [[CrossRef](#)]
42. Enenkel, M.; Farah, C.; Hain, C.; White, A.; Anderson, M.; You, L.; Wagner, W.; Osgood, D. What Rainfall Does Not Tell Us—Enhancing Financial Instruments with Satellite-Derived Soil Moisture and Evaporative Stress. *Remote Sens.* **2018**, *10*, 1819. [[CrossRef](#)]
43. Jonah, K.; Wen, W.; Shahid, S.; Ali, A.; Bilal, M.; Habtemicheal, B.A.; Iyakaremye, V.; Qiu, Z.; Almazroui, M.; Wang, Y.; et al. Spatiotemporal variability of rainfall trends and influencing factors in Rwanda. *J. Atmos. Sol.-Terr. Phys.* **2021**, *219*, 105631. [[CrossRef](#)]

44. Ndakize Joseph, S.; Frederic, N.; Aminadab, T.; Vedaste, I. A Statistical Analysis of the Historical Rainfall Data Over Eastern Province in Rwanda. *East Afr. J. Sci. Technol.* **2020**, *10*, 33–52.
45. Bazambanza, A. Study of the Performance of a Regional Climate Model in Simulating Rainfall in Rwanda. Ph.D. Thesis, University of Rwanda, Kigali, Rwanda, 2022.
46. Olaka, L.A.; Ogotu, J.O.; Said, M.Y.; Oludhe, C. Projected Climatic and Hydrologic Changes to Lake Victoria Basin Rivers under Three RCP Emission Scenarios for 2015–2100 and Impacts on the Water Sector. *Water* **2019**, *11*, 1449. [[CrossRef](#)]
47. Manners, R.; Vandamme, E.; Adewopo, J.; Thornton, P.; Friedmann, M.; Carpentier, S.; Ezui, K.S.; Thiele, G. Suitability of root, tuber, and banana crops in Central Africa can be favoured under future climates. *Agric. Syst.* **2021**, *193*, 103246. [[CrossRef](#)]
48. Balagizi, C.M.; Kasereka, M.M.; Cuoco, E.; Liotta, M. Rain-plume interactions at Nyiragongo and Nyamulagira volcanoes and associated rainwater hazards, East Africa. *Appl. Geochem.* **2017**, *81*, 76–89. [[CrossRef](#)]
49. Fessehaye, M.; Franke, J.; Brönnimann, S. Evaluation of satellite-based (CHIRPS and GPM) and reanalysis (ERA5-Land) precipitation estimates over Eritrea. *Meteorol. Z.* **2022**, *31*, 401–413. [[CrossRef](#)]
50. Harrison, L.; Landsfeld, M.; Husak, G.; Davenport, F.; Shukla, S.; Turner, W.; Peterson, P.; Funk, C. Advancing early warning capabilities with CHIRPS-compatible NCEP GFS precipitation forecasts. *Sci. Data* **2022**, *9*, 375. [[CrossRef](#)]
51. Nkrumah, F.; Quagraine, K.A.; Quagraine, K.T.; Wainwright, C.; Quenum, G.M.L.D.; Amankwah, A.; Klutse, N.A.B. Performance of CMIP6 HighResMIP on the Representation of Onset and Cessation of Seasonal Rainfall in Southern West Africa. *Atmosphere* **2022**, *13*, 999. [[CrossRef](#)]
52. Pervez, S.; McNally, A.; Arsenault, K.; Budde, M.; Rowland, J. Vegetation Monitoring Optimization with Normalized Difference Vegetation Index and Evapotranspiration Using Remote Sensing Measurements and Land Surface Models Over East Africa. *Front. Clim.* **2021**, *3*, 589981. [[CrossRef](#)]
53. Muhire, I.; Tesfamichael, S.; Ahmed, F.; Minani, E. Spatio-temporal trend analysis of projected precipitation data over Rwanda. *Theor. Appl. Clim.* **2016**, *131*, 671–680. [[CrossRef](#)]
54. Kamau-Muthoni, F.; Omondi-Odongo, V.; Ochieng, J.; Mugalavai, E.M.; Kjumula-Mourice, S.; Hoesche-Zeledon, I.; Mwila, M.; Bekunda, M. Long-term spatial-temporal trends and variability of rainfall over eastern and Southern Africa. *Theor. Appl. Climatol.* **2019**, *137*, 1869–1882. [[CrossRef](#)]
55. Muhire, I.; Ahmed, F. Spatio-temporal trend analysis of precipitation data over Rwanda. *S. Afr. Geogr. J.* **2014**, *97*, 50–68. [[CrossRef](#)]
56. Aguilera, E.; Diaz-Gaona, C.; Garcia-Laureano, R.; Reyes-Palomo, C.; Guzman, G.; Ortolani, L.; Sanchez-Rodriguez, M.; Rodriguez-Estevez, V. Agroecology for adaptation to climate change and resource depletion in the Mediterranean region. A review. *Agric. Syst.* **2020**, *181*, 102809. [[CrossRef](#)]
57. Farjami, H.; Hesari, A.R.E. Assessment of sea surface wind field pattern over the Caspian Sea using EOF analysis. *Reg. Stud. Mar. Sci.* **2020**, *35*, 101254. [[CrossRef](#)]
58. Umutoni, M.; Limbu, P. Characteristics of Extreme Precipitation and Their Effect on Bean Yield in Rwanda. *Tanzan. J. Eng. Technol.* **2022**, *41*, 24–42. [[CrossRef](#)]
59. Mbatia, M. Towards Improving the Skill of Seasonal Rainfall Prediction over Rwanda. Ph.D. Thesis, University of Nairobi, Nairobi, Kenya, 2019.
60. Ngoma, H.; Wen, W.; Ayugi, B.; Karim, R.; Kisesa, M.E. Mechanisms associated with September to November (SON) rainfall over Uganda during the recent decades. *Geogr. Pannonica* **2021**, *25*, 10–23. [[CrossRef](#)]
61. Babaousmail, H.; Ayugi, B.O.; Onyutha, C.; Kebacho, L.L.; Ojara, M.; Ongoma, V. Analysis of Changes in Rainfall Concentration over East Africa. *Atmosphere* **2023**, *14*, 1679. [[CrossRef](#)]
62. Nkunuzimana, A.; Bi, S.; Jiang, T.; Wu, W.; Abro, M.I. Spatiotemporal variation of rainfall and occurrence of extreme events over Burundi during 1960 to 2010. *Arab. J. Geosci.* **2019**, *12*, 176. [[CrossRef](#)]
63. Onyutha, C. Analyses of rainfall extremes in East Africa based on observations from rain gauges and climate change simulations by CORDEX RCMs. *Clim. Dyn.* **2020**, *54*, 4841–4864. [[CrossRef](#)]
64. Nkurunziza, I.F.; Guirong, T.; Ngarukiyimana, J.P.; Sindikubwabo, C. Influence of the Mascarene High on October–December rainfall and their associated atmospheric circulation anomalies over Rwanda. *J. Environ. Agric. Sci.* **2019**, *20*, 1–20.
65. Ayabagabo, P. Empirical Analysis of Seasonal Rainfall Variability and Its Associated Effects on Major Food Crop Yields in Rwanda. Ph.D. Thesis, University of Nairobi, Nairobi, Kenya, 2018.
66. Cattani, E.; Merino, A.; Guijarro, J.A.; Levizzani, V. East Africa Rainfall Trends and Variability 1983–2015 Using Three Long-Term Satellite Products. *Remote Sens.* **2018**, *10*, 931. [[CrossRef](#)]
67. Safari, B.; Sebaziga, J.N.; Siebert, A. Evaluation of CORDEX-CORE regional climate models in simulating rainfall variability in Rwanda. *Int. J. Clim.* **2022**, *43*, 1112–1140. [[CrossRef](#)]
68. Ngarukiyimana, J.P.; Fu, Y.; Yang, Y.; Ogwang, B.A.; Ongoma, V.; Ntwali, D. Dominant Atmospheric Circulation Patterns Associated with Abnormal Rainfall Events over Rwanda, East Africa. *Int. J. Climatol.* **2018**, *38*, 187–202. [[CrossRef](#)]
69. Sebaziga Ndakize, J. Spatial-Temporal Variability and Projected Rainfall over Rwanda. Doctoral Dissertation, University of Rwanda, Kigali, Rwanda, 2018.
70. Siebert, A.; Dinku, T.; Vuguziga, F.; Twahirwa, A.; Kagabo, D.M.; Delcorral, J.; Robertson, A.W. Evaluation of ENACTS-Rwanda: A new multi-decade, high-resolution rainfall and temperature data set—Climatology. *Int. J. Clim.* **2019**, *39*, 3104–3120. [[CrossRef](#)]
71. Bhaga, T.D.; Dube, T.; Shekede, M.D.; Shoko, C. Impacts of Climate Variability and Drought on Surface Water Resources in Sub-Saharan Africa Using Remote Sensing: A Review. *Remote Sens.* **2020**, *12*, 4184. [[CrossRef](#)]

72. Chang'a, L.B.; Kijazi, A.L.; Mafuru, K.B.; Nying'uro, P.A.; Ssemujju, M.; Deus, B.; Kondowe, A.L.; Yonah, I.B.; Ngwali, M.; Kisama, S.Y.; et al. Understanding the Evolution and Socio-Economic Impacts of the Extreme Rainfall Events in March–May 2017 to 2020 in East Africa. *Atmos. Clim. Sci.* **2020**, *10*, 553–572. [[CrossRef](#)]
73. Umuhoza, J.; Chen, L.; Mumo, L. Assessing the Skills of Rossby Centre Regional Climate Model in Simulating Observed Rainfall over Rwanda. *Atmos. Clim. Sci.* **2021**, *11*, 398–418. [[CrossRef](#)]
74. Ntikubitubugingo, E. Future rainfall projections for Rwanda using statistical downscaling. Master's Thesis, University of Rwanda, Kigali, Rwanda, 2018.
75. Nkuzimana, A.; Bi, S.; Alriah, M.A.A.; Zhi, T.; Kur, N.A.D. Diagnosis of meteorological factors associated with recent extreme rainfall events over Burundi. *Atmos. Res.* **2020**, *244*, 105069. [[CrossRef](#)]

Disclaimer/Publisher's Note: The statements, opinions and data contained in all publications are solely those of the individual author(s) and contributor(s) and not of MDPI and/or the editor(s). MDPI and/or the editor(s) disclaim responsibility for any injury to people or property resulting from any ideas, methods, instructions or products referred to in the content.